Bioorg. Med. Chem. 39 (2021) 116141

Contents lists available at ScienceDirect

Bioorganic & Medicinal Chemistry

journal homepage: www.elsevier.com/locate/bmc

SAR insights into TET2 catalytic domain inhibition: Synthesis of 2-Hydroxy-4-Methylene-pentanedicarboxylates

Anand D. Tiwari [a,*], Yihong Guan [a], Dale R. Grabowski [a], Jaroslaw P. Maciejewski [a,b,c], Babal K. Jha [a,b,c], James G. Phillips [a,c,*]

[a] Department of Translational Hematology and Oncology Research, Taussig Cancer Institute, Cleveland, OH 44195, USA
[b] Cleveland Clinic Lerner College of Medicine, Cleveland, OH 44195, USA
[c] Case Comprehensive Cancer Center, Case Western Reserve University, Cleveland, OH 44106, USA

ARTICLE INFO

Keywords:
TET
Dioxygenase
2-Hydroxyglutarate
Epigenetic
Enzyme inhibition
α-KG

ABSTRACT

The TET (Ten-Eleven Translocation) dioxygenase enzyme family comprising 3 members, TET1-3, play key roles in DNA demethylation. These processes regulate transcription programs that determine cell lineage, survival, proliferation, and differentiation. The impetus for our investigations described here is derived from the need to develop illuminating small molecule probes for TET enzymes with cellular activity and specificity. The studies were done so in the context of the importance of TET2 in the hematopoietic system and the preponderance of loss of function somatic TET2 mutations in myeloid diseases. We have identified that 2-hydroxy-4-methylene-pentanedicarboxylic acid **2a** reversibly competes with the co-substrate α-KG in the TET2 catalytic domain and inhibits the dioxygenase activity with an $IC_{50} = 11.0 \pm 0.9$ μM at 10 μM α-KG in a cell free system and binds in the TET2 catalytic domain with $K_d = 0.3 \pm 0.12$ μM.

1. Introduction

The Ten-Eleven Translocation (TET1-3) enzyme family are DNA hydroxylases which effect DNA demethylation, and thereby the propagation and preservation of epigenetic information.[1,2] Methylation and demethylation patterns of enhancer and promoter CpG islands establish transcription programs that determine cell lineage, survival, and proliferation.[3] The C-terminal catalytic domain of the three TET1-3 enzymes is highly conserved and supports the oxidizing function of TETs by employing oxygen, Fe(II), and α-ketoglutarate (α-KG) to mediate DNA demethylation via successive oxidation of 5-methylcytosine (5mC) to 5-hydroxymethylcytosine (5hmC), 5-formylcytosine (5fC), and finally 5-carboxycytosine (5caC).[4] The higher oxidized bases, 5fC and 5caC, can be removed from the DNA base sequence by base excision repair mechanisms, and replaced by cytosine in the DNA sequence.[5] Pertinent to our efforts described here is the importance of TET2 in the hematopoietic system illuminated by identification of somatic mutations of this gene in myeloid and lymphoid neoplasia and in clonal hematopoiesis of indeterminate potential (CHIP), a condition associated with higher risk of developing subsequent myeloid malignancy and cardiovascular disorders.[6,7] These loss of function or hypomorphic mutations indicate that TET2 is a bona fide tumor suppressor gene.[8] Although, there is growing support that temporarily inhibiting TET2 activity may be beneficial in certain contexts, there are no discerning small molecules available to study that task. Therefore, we felt obliged to undertake investigations to more rigorously probe the potential of inhibiting TET2 dioxygenase

Abbreviations: TET, Ten-Eleven Translocation Proteins; DNA, Deoxyribose nucleic acid; α-KG, α-ketoglutarate; Fe, Iron; 5mC, 5-methylcytosine; 5hmC, 5-hydroxymethylcytosine; 5fC, 5-formylcytosine; 5caC, 5-carboxycytosine; TDG, thymine DNA glycosylase; CHIP, clonal hematopoiesis of indeterminate potential; NOG, *N*-oxalylglycine; NMR, Nuclear magnetic Resonance spectroscopy; ppm, part per million; *J*, coupling constants; br s, broad singlet; D, doublet; Dd, doublet of doublets; Ddd, doublet of doublet of doublets; br d, broad doublets; t, triplet; dt, triplets of doublets; q, quartet; m, multiplet; br m, broad multiplet; DMSO, dimethyl sulfoxide; THF, tetrahydrofuran; HPLC, high performance liquid chromatography; EtOAc, ethyl acetate; MeCN, acetonitrile; UV, ultra violet; d, deuterated; PBS, phosphate buffer solution; h, hour; min, minutes; LiOH, lithium hydroxide; DIPEA. N, N, diisopropyl ethyl amine; DMAP, dimethyl amino pyridine; EDTA, Ethylenediaminetetraacetic acid; TBST, tris-buffered saline; ELISA, enzyme-linked immunosorbent assay; IDT, Integrated DNA Technologies; HEPES, N-2-hydroxyethylpiperazine-*N*-ethanesulfonic acid; BSA, bovine serum albumin.

* Corresponding authors at: 9500 Euclid Avenue, NE6-307, Cleveland, OH 44195, United States (J. Phillips). 9500 Euclid Avenue, NE6-255, Cleveland, OH, 44195, United States (A. Tiwari).

E-mail addresses: tiwaria@ccf.org (A.D. Tiwari), phillij5@ccf.org (J.G. Phillips).

https://doi.org/10.1016/j.bmc.2021.116141
Received 23 January 2021; Received in revised form 25 March 2021; Accepted 27 March 2021
Available online 20 April 2021

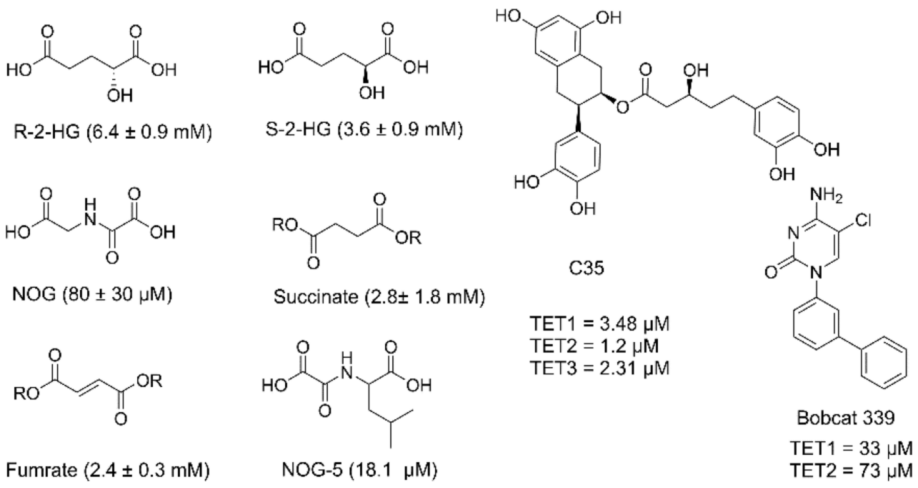

Figure 1. The apparent IC_{50} values of some small molecule TET inhibitors.

function via its catalytic domain.

Early studies have shown that small molecules that competitively bind in the TET catalytic site in similar fashion as the co-substrate α-KG but are not poised to undergo oxidative decarboxylation inhibit the TET catalytic cycle.[9] For example, in the presence of 0.1 mM of α-KG, addition of 10 mM or 50 mM *R*-2-hydroxyglutarate (*R*-2-HG), resulted in 33% and 83% inhibition of TET2, respectively. *R*-2-HG exhibited a less pronounced inhibitory effect toward TET1, reducing the 5hmC production by 28% and 47%, respectively, when 10 and 50 mM *R*-2-HG were used. *S*-2-HG was found to be more potent than *R*-2-HG in inhibiting both TET2 and TET1 with 10 mM *S*-2-HG capable of inhibiting most of TET1 and TET2 activity in the presence of 0.1 mM α-KG. These results demonstrate that both enantiomers *R*-2-HG and *S*-2-HG are weak inhibitors of TET dioxygenases.[10] In the same study, they have also been disclosed as weak non-selective competitive inhibitors of multiple α-KG dependent dioxygenases and histone demethylases. Other small molecules have been demonstrated to be catalytic domain inhibitors of TET proteins. Figure 1 shows the IC_{50} values for several small molecule TET catalytic domain inhibitors reported recently. For instance, *N*-oxalylglycine (NOG), an α-KG analog, has been described as a non-specific inhibitor of α-KG utilizing enzymes, but significantly a more potent TET inhibitor than either enantiomer of 2-HG. In this regard, an x-ray crystal structure of NOG bound in the catalytic site of a truncated domain TET2 protein-DNA complex provides useful insight into TET mediated 5mC oxidation and perhaps future drug design.[11] Mutant specific *N*-oxalylglycine (NOG) derived inhibitors have been developed through a 'bump-and-hole' strategy.[12] By genetically engineering in certain mutations of bulky hydrophobic amino acid residues that help bind α-KG in the catalytic site, a series of NOG analogs bearing alkyl and aryl moieties at the carbon α to the amide nitrogen of NOG were developed. The NOG-5 derivative with an isobutyl substituent (Figure 1) was an effective inhibitor (IC_{50} = 18.1 μM) against a double TET2 mutant with no effect on the wild type (WT)-TET2.[13]

Two other recently reported efforts to develop TET enzyme inhibitors are worthy of note. Bobcat 339 (Figure 1), a novel N-1-biphenyl-5-chloro substituted cytosine, was shown to dose dependently inhibit both TET1 (IC_{50} = 33 μM) and TET2 (IC_{50} = 73 μM).[14] A molecular modeling screening campaign of the National Cancer Institute compound library (265,000 compounds) identified C35 (Figure 1) which was subsequently shown *in vitro* to inhibit TET1-3 with IC_{50} = 3.48, 1.2, and 2.31 μM, respectively.[15]

Despite progress in delineating the importance of TET enzymes and their significance in disease maintenance when mutated or deregulated, the therapeutic options to restore or modulate appropriate TET activity are currently lacking. Our studies here were initiated to examine in more detail the effect of other small molecules related to α-KG and NOG on TET catalytic domain function. For this purpose, we considered combining two features learned from the published inhibitors mentioned into our design of novel 2,4-disubstituted pentanedicarboxylic acids: Compounds that cannot undergo oxidative decarboxylation inhibit the TET catalytic cycle, i.e., NOG contains a C-2 amide carbonyl in place of the reactive C-2 carbonyl as in α-KG. Substitution of a hydroxyl group for the carbonyl functionality at position C-2 as in 2-HG also appears to inhibit the cycle. We therefore considered an orthogonal methylene substituent at C-4 as a feature to prevent oxidative decarboxylation combined with a secondary or tertiary C-2 hydroxy group to synthesize catalytic domain TET2 inhibitors.

2. Materials and methods

2.1. Chemistry experimental

2.1.1. General procedures

All chemicals and reagents were used as received without further purification. Glassware was dried in an oven at 100 °C and purged with a dry N_2 atmosphere prior to use. Unless mentioned, reactions were performed open to air. Reactions were monitored by TLC and visualized by a dual short/long wavelength UV lamp and potassium permanganate solution. Flash column chromatography was performed using silica gel (60–200 μ, 60 A, Dynamic Adsorbent). NMR spectra were recorded on a 500/400 MHz Bruker Ascend Avance III HD at room temperature. Chemical shifts for ^{1}H, and ^{13}C NMR were reported as δ, part per million (ppm), and referenced to an internal deuterated solvent central line or TMS. Multiplicity and coupling constants (*J*) were calculated automatically on MestReNova 11.0, NMR processing software from Mestrelab Research. The purity of the newly synthesized compounds (>95%) were determined by NMR. High Resolution Mass Spectrometry (HRMS-ESI) mass spectra were acquired on an Agilent Q-TOF. Circular dichroism spectra were recorded on the JASCO J-815CD spectrometer. Specific optical rotation ($[\alpha]^{20}_{D}$) were observed using sodium D-line (λ = 589 nm) in Anton Parr MC 200 with a 50 mm cell.

2.1.2. General synthesis method for the Barbier reaction

To a suspension of activated zinc powder (1.5 mol equiv.) in 50 mL dry acetonitrile was added acetic acid (1.5 mol equiv.). Ethyl 2-bromoacrylate (1 mol equiv.) was added to the reaction mixture followed by the drop wise addition of aldehyde or ketone (1.1 mol equiv.). The reaction mixture was stirred at 20 °C for 6–12 h. The reaction was monitored by TLC for completion (Potassium permanganate staining). The mixture was filtered through celite and the filtrate evaporated under reduced pressure. The residue was dissolved in 100 mL ethyl acetate and the organic layer washed with 50 mL of saturated aqueous ammonium

chloride solution followed by brine, separated, and dried over sodium sulfate. Filtration and evaporation under reduced pressure provided the crude products as oils. Flash silica gel column chromatography eluting with 7–12% ethyl acetate: hexanes provided desired products in 45–95% yields in > 95% purity. All new compounds were fully characterized by ^{1}H, ^{13}C NMR, and HRMS.

*Diethyl 2-hydroxy-4-methylenepentanedioate (**1a**):* The obtained compound was a clear oil, yield 95%. ^{1}H NMR (500 MHz, Chloroform-d) δ 6.29 (d, J = 1.3 Hz, 1H), 5.72 (q, J = 1.1 Hz, 1H), 4.42 – 4.37 (m, 1H), 4.23 (qd, J = 7.1, 5.5 Hz, 4H), 3.13 (d, J = 5.5 Hz, 1H), 2.86 (ddd, J = 14.2, 4.5, 1.2 Hz, 1H), 2.64 (ddd, J = 14.3, 8.1, 1.0 Hz, 1H), 1.31 (q, J = 7.2 Hz, 6H). ^{13}C NMR (126 MHz, CDCl3) δ 174.4, 167.2, 136.0, 128.4, 69.7, 61.8, 61.2, 37.4, 14.3.14.2 HRMS (ESI +) *m/z* 239.0887 [M + Na]$^{+}$; calculated for $C_{10}H_{16}O_5$ [M + Na]$^{+}$ 239.0890.

*Diethyl 2-hydroxy-2-methyl-4-methylenepentanedioate (**1b**):* The compound was a clear oil, yield 80%. ^{1}H NMR (400 MHz, Chloroform-*d*) δ 6.27 (d, J = 1.7 Hz, 1H), 5.68 (d, J = 1.8 Hz, 1H), 4.27 – 4.10 (m, 4H), 3.60 (s, 1H), 2.85 (d, J = 13.9, 1H), 2.68 (dd, J = 13.9, 1H), 1.44 (s, 3H), 1.30 (td, J = 7.1, 4.6 Hz, 6H). ^{13}C NMR (100 MHz, $CDCl_3$) δ 176.0, 167.8, 135.9, 128.9, 74.3, 61.9, 61.2, 42.0, 25.7, 14.3(2C). HRMS (ESI +) *m/z* 231.1229 [M + H]$^{+}$; calculated for $C_{11}H_{18}O_5$ [M + H]$^{+}$ 231.1227.

*Diethyl 2-hydroxy-4-methylene-2-(trifluoromethyl)pentanedioate (**1c**):* The compound was a clear oil, yield 60%. ^{1}H NMR (400 MHz, Chloroform-*d*) δ 6.32 (d, J = 1.3 Hz, 1H), 5.78 (s, 1H), 4.39 (s, 1H), 4.37 – 4.32 (m, 1H), 4.28 (ddd, J = 10.5, 7.0, 3.3 Hz, 1H), 4.22 (qd, J = 7.1, 2.8 Hz, 2H), 3.12 (d, J = 14.3 Hz, 1H), 2.95 (d, J = 14.3 Hz, 1H), 1.32 (dt, J = 9.6, 7.1 Hz, 6H). ^{13}C NMR (100 MHz, $CDCl_3$) δ 168.7, 167.4, 133.4, 130.2, 124.5, 122.2, 63.6, 61.5, 33.8, 33.7, 14.1, 13.9. ^{19}F NMR (376 MHz, $CDCl_3$) δ −78.41. HRMS (ESI +) *m/z* 285.0947 [M + H]$^{+}$; calculated for $C_{11}H_{15}F_3O_5$ [M + H]$^{+}$ 285.0944.

*Diethyl 2-ethyl-2-hydroxy-4-methylenepentanedioate (**1d**):* The compound was a clear oil, 65% yield. ^{1}H NMR (400 MHz, Chloroform-*d*) δ 6.22 (d, J = 1.7 Hz, 1H), 5.65 (d, J = 1.9 Hz, 1H), 4.28 – 4.09 (m, 4H), 3.53 (s, 1H), 2.80 (d, J = 14.0 Hz, 1H), 2.70 (d, J = 13.9 Hz, 1H), 1.85 (dt, J = 14.5, 7.2 Hz, 1H), 1.68 (dd, J = 14.7, 7.5 Hz, 1H), 1.28 (td, J = 7.2, 1.7 Hz, 6H), 0.87 (t, J = 7.4 Hz, 3H). ^{13}C NMR (101 MHz, $CDCl_3$) δ 175.6, 167.8, 136.1, 128.5, 77.6, 61.8, 61.1, 40.9, 32.1, 14.4, 14.3, 8.0. HRMS (ESI +) *m/z* 267.1198 [M + Na]$^{+}$; calculated for $C_{12}H_{20}O_5$ [M + Na]$^{+}$ 267.1203.

*Diethyl 2-hydroxy-2-isopropyl-4-methylenepentanedioate (**1e**):* This compound was obtained as clear oil, yield 45%. ^{1}H NMR (400 MHz, Chloroform-*d*) δ 6.18 (d, J = 1.7 Hz, 1H), 5.64 (s, 1H), 4.27 – 4.08 (m, 4H), 3.52 (s, 1H), 2.87 – 2.78 (m, 1H), 2.74 (d, J = 14.0 Hz, 1H), 2.05 (p, J = 6.8 Hz, 1H), 1.29 (td, J = 7.2, 4.5 Hz, 6H), 1.01 (d, J = 6.9 Hz, 3H), 0.88 (d, J = 6.8 Hz, 3H). ^{13}C NMR (101 MHz, $CDCl_3$) δ 175.7, 168.0, 136.8, 127.9, 80.0, 61.7, 61.1, 38.5, 35.7, 17.6, 16.1, 14.3, 14.2. HRMS (ESI +) *m/z* 281.1354 [M + Na]$^{+}$; calculated for $C_{13}H_{22}O_5$ [M + Na]$^{+}$ 281.1359.

*Ethyl 4-hydroxy-2-methylenepentanoate (**1f**):* This compound was a white amorphous powder, yield 55%. ^{1}H NMR (400 MHz, Chloroform-*d*) δ 6.26 (d, J = 1.7 Hz, 1H), 5.66 (d, J = 1.8 Hz, 1H), 4.22 (q, J = 7.2 Hz, 2H), 4.00 – 3.94 (m, 1H), 2.56 (dd, J = 14.0, 3.9 Hz, 1H), 2.38 (dd, J = 13.9, 8.0 Hz, 1H), 2.18 (d, J = 6.0, 1H), 1.31 (t, J = 7.2, 3H), 1.22 (d, J = 6.3, 3H). ^{13}C NMR (100 MHz, $CDCl_3$) δ 167.8, 137.8, 127.7, 67.0, 61.2, 42.1, 23.2, 14.3. HRMS (ESI +) *m/z* 159.1013 [M + H]$^{+}$; calculated for $C_8H_{14}O_3$ [M + H]$^{+}$ 159.1016.

2.1.3. General method for saponification of diesters with aqueous lithium hydroxide

The diesters (1.0 mmol) were saponified with lithium hydroxide (LiOH, 1.0 M aqueous, 2–3 mol equiv.) in THF (50 mL) at 20 °C for 6 h with continuous stirring. Reactions were monitored by TLC for completion. The crude reaction was concentrated under reduced pressure and residue dissolved in 50 mL water and pH adjusted with 10% HCl (1.2 M) till pH 4.0. The aqueous solution at pH 4.0 was washed with ethyl acetate (50 mL) once, separated, and then water was removed by lyophilization. Sep-Pak C-18 reverse phase column chromatography was used for further purification in acetonitrile:water (8:2). Pure diacid powders were obtained by lyophilization.

*2-Hydroxy-4-methylenepentanedioic acid (**2a**):* The compound obtained as a white crystalline solid, yield 55%. ^{1}H NMR (400 MHz, Deuterium Oxide) ^{1}H NMR (400 MHz, Deuterium Oxide) δ 6.02 (d, J = 1.5 Hz, 1H), 5.61 – 5.57 (m, 1H), 4.20 (dd, J = 8.5, 4.0 Hz, 1H), 2.8 – 2.75 (m, 1H), 2.54 (dd, J = 14.5, 8.5 Hz, 1H). ^{13}C NMR (101 MHz, D_2O) δ 180.3, 174.1, 139.8, 125.4, 71.4, 37.4. HRMS (ESI-): *m/z* 159.0294 [M−H]$^{-}$; calculated for $C_6H_8O_5$ [M−H]$^{-}$ 159.0299.

*2-Hydroxy-2-methyl-4-methylenepentanedioic acid (**2b**):* The compound was obtained as an off white crystalline solid, yield 60%. ^{1}H NMR (500 MHz, Methanol-d_4) δ 6.02 (d, J = 2.3 Hz, 1H), 5.44 (d, J = 2.2 Hz, 1H), 3.35 (s, 1H), 2.72 (q, J = 13.7 Hz, 2H), 1.33 (s, 3H). ^{13}C NMR (126 MHz, MeOD) δ 183.0, 175.9, 143.0, 125.5, 77.5, 44.0, 26.9. HRMS (ESI-): *m/z* 173.0451 [M−H]$^{-}$; calculated for $C_7H_{10}O_5$ [M−H]$^{-}$ 173.0455.

*2-Hydroxy-4-methylene-2-(trifluoromethyl)pentanedioic acid (**2c**)*: The obtained compound was an off white solid, yield 40%. ^{1}H NMR (400 MHz, Deuterium Oxide) δ 5.95 (d, J = 1.5 Hz, 1H), 5.51 (s, 1H), 2.97 – 2.85 (m, 2H). ^{13}C NMR (101 MHz, D_2O) δ 175.7, 173.3, 138.9, 126.1, 125.4, 123.2, 78.8, 78.6, 34.9. HRMS (ESI-): *m/z* 227.0170 [M−H]$^{-}$; calculated for $C_7H_7F_3O_5$ [M−H]$^{-}$ 227.0173.

2.1.4. Dess-Martin oxidation of selected alcohols

The hydroxy derivatives were dissolved in dichloromethane (50 mL) in a 100 mL round bottom flask and Dess-Martin-Periodinane (1.5 equiv. mol ratio) was added to the solution. The heterogeneous mixture was stirred at 20 °C for 4 h. The reaction was monitored by TLC for the complete oxidation of hydroxy derivative. The solvent was evaporated under reduced pressure and residue was dissolved in ethyl acetate (100 mL). The organic layer was washed with 1:1 $NaHCO_3$ (10%) and $Na_2S_2O_3$ (10%) aqueous solution twice (50 mL each). The organic layer again washed with brine solution (50 mL) and dried over the sodium sulfate, filtered and solvent were evaporated under reduced pressure. The crude compounds were purified by the flash silica column chromatography and obtained in 80–90% yields.

*Diethyl 2-methylene-4-oxopentanedioate (**3a**):* Off white solid, yield 80%. ^{1}H NMR (500 MHz, Chloroform-d) δ 6.39 (s, 1H), 5.70 (s, 1H), 4.33 (q, J = 7.1 Hz, 2H), 4.19 (q, J = 7.2 Hz, 2H), 3.82 (s, 2H), 1.36 (t, J = 7.2 Hz, 3H), 1.27 (t, J = 7.2 Hz, 3H).

*Ethyl 1-(3-ethoxy-2,3-dioxopropyl)cyclopropane-1-carboxylate (**7a**):* Off white solid, yield 80%. ^{1}H NMR (500 MHz, Chloroform-*d*) δ 4.33 (q, J = 7.2 Hz, 2H), 4.09 (q, J = 7.1 Hz, 2H), 3.04 (s, 2H), 1.40 – 1.37 (m, 4H), 1.31 – 1.20 (m, 5H), 1.19 (t, J = 7.1 Hz, 3H), 0.82 (q, J = 4.4 Hz, 2H). ^{13}C NMR (126 MHz, $CDCl_3$) δ 192.3, 174.0, 161.3, 62.6, 61.12, 43.3, 19.7, 18.0, 15.4, 14.3, 14.12, 14.1.

*Ethyl 1-(3-ethoxy-2-hydroxy-3-oxopropyl)cyclopropane-1-carboxylate (**5a**):* This derivative was synthesized according to previously published literature.[16] Clear oil, yield 45%. ^{1}H NMR (500 MHz, Chloroform-*d*) δ 4.42 (dt, J = 9.3, 4.5 Hz, 1H), 4.23 (dtd, J = 21.1, 7.1, 3.6 Hz, 2H), 4.12 (q, J = 7.1 Hz, 2H), 3.39 (d, J = 6.2 Hz, 1H), 2.09 (dd, J = 14.7, 4.2 Hz, 1H), 1.90 (dd, J = 14.7, 8.7 Hz, 1H), 1.30 (t, J = 7.1 Hz, 3H), 1.24 (t, J = 7.2 Hz, 3H), 0.91 (ddd, J = 9.7, 6.6, 3.8 Hz, 1H), 0.79 – 0.72 (m, 1H). ^{13}C NMR (126 MHz, $CDCl_3$) δ 175.6, 174.9, 70.4, 61.6, 61.0, 39.1, 21.3, 16.2, 15.4, 14.3.

*Diethyl 2-fluoro-4-methylenepentanedioate (**8a**)*: This derivative was synthesized according to previously published literature.[16] ^{1}H NMR (500 MHz, Chloroform-*d*) δ 6.34 (s, 1H), 5.76 (s, 1H), 5.16 – 5.04 (m, 1H), 4.44 (q, J = 7.2 Hz, 1H), 4.24 (dt, J = 14.8, 7.0 Hz, 3H), 2.99 (ddd, J = 29.5, 14.7, 4.2 Hz, 1H), 2.82 (td, J = 16.3, 15.4, 8.6 Hz, 1H), 1.44 (t, J = 7.2 Hz, 1H), 1.34 – 1.28 (m, 4H), 1.25 (d, J = 5.1 Hz, 1H).

2.1.5. General Pd/C hydrogenation of selected 4-methylene pentanedicarboxylate esters

Selected 4-methylene derivatives were reduced in 50 mL absolute

ethanol in a Parr hydrogenation vessel using a catalytic amount of Palladium hydroxide ($Pd(OH)_2$), 20 wt% Pd (dry basis), on carbon (Aldrich, 212111, 0.1 equiv. mol ratio). The reaction vessel was deoxygenated prior to the reaction and H_2 pressure was kept at 30–40 psi for 2 h until completion of the reaction. The reaction mixture was filtered through celite and the filtrate evaporated under reduced pressure. Crude products were purified by flash silica column chromatography and obtained as oils in good yield (80–90%).

Diethyl 2-hydroxy-4-methylpentanedioate (**4a**)*:* Clear oil, yield 60%. ^{1}H NMR (400 MHz, Chloroform-*d*) δ 4.31 – 4.08 (m, 5H), 2.87 (d, J = 29.6 Hz, 1H), 2.79 – 2.67 (m, 1H), 2.27 – 1.99 (m, 1H), 1.90 – 1.62 (m, 1H), 1.35 – 1.16 (m, 9H).^{13}C NMR (101 MHz, $CDCl_3$) δ (176.5, 176.3), (175.1, 175.0), (68.9, 68.7), (62.0, 61.9), (60.6, 60.6), (38.2, 37.9), (36.1, 35.9), 18.0, 16.8, (14.32, 14.3). HRMS (ESI +) *m/z* 219.1247 $[M + H]^+$; calculated for $C_{10}H_{18}O_5$ $[M + H]^+$ 219.1227.

Diethyl 2,2-difluoro-4-methylpentanedioate (**14**)*:* Clear oil, yield 70%. ^{1}H NMR (500 MHz, Chloroform-*d*) δ 4.32 (q, J = 7.2 Hz, 2H), 4.15 (q, J = 7.2 Hz, 2H), 2.82 – 2.74 (m, 1H), 2.64 (dtd, J = 22.1, 14.4, 7.9 Hz, 1H), 2.11 (dtd, J = 20.1, 14.4, 5.2 Hz, 1H), 1.36 (d, J = 7.2 Hz, 3H), 1.26 (t, J = 6.8 Hz, 6H).

*Synthesis of Dimethyl 2-chloro-4-methylenepentanedioate (**9**):* Methyl 2-(hydroxymethyl)acrylate (5.0 g, 43.06 mmol), d = 1.13 g/mL) and 2-Chloro-1,1,1-ethoxyethane (8.0 mL, 51.67 mmol, d = 1.15 g/mL) were added together in 200 mL round bottom flask with 100 mL toluene and catalytic amount acetic acid (1 mL, 4.31 mmol). The reaction mixture was refluxed for 24 h at 130 °C. The completion of reaction was monitored by TLC. The reaction mixture was subjected to azeotropic distillation with toluene under reduced pressure (3x50 mL) to provide the desired compound obtained as a yellow oil and used as such without further purification, yield 85%. ^{1}H NMR (500 MHz, Chloroform-*d*) δ 6.32 (s, 1H), 5.74 (s, 1H), 4.54 (dd, J = 8.2, 6.4 Hz, 1H), 3.76 (s, 6H), 3.06 (dd, J = 14.3, 6.3 Hz, 1H), 2.82 (dd, J = 14.2, 8.3 Hz, 1H). ^{13}C NMR (126 MHz, $CDCl_3$) δ 169.7, 166.6, 134.7, 130.1, 54.9, 53.0, 52.2, 37.9. HRMS (ESI-): *m/z* 207.0414 $[M + H]^+$; calculated for $C_8H_{11}ClO_4$ $[M + H]^+$ 207.0419.

*2-Hydroxy-4-methylenepentanedioic acid (**10/2a**):* Compound **9** (0.450 g, 2.18 mmol) was dissolved in 30 mL THF, aqueous lithium hydroxide (1.0 M, 4.5 mL) was added and stirred for 4 h at 20 °C. The reaction mixture was evaporated under reduced pressure and residue was dissolved in 20 mL water, acidified to pH 4.0 with 10% HCl (1.2 M), and washed with ethyl acetate (50 mL) once. Water was removed by lyophilization. The obtained solid was dissolved in 25% acetonitrile/ water solution. The solution was passed through a Sep-Pak (5G) reverse phase column eluting with water followed by 20% acetonitrile/water. The pure fractions were lyophilized and gave **2a** as product. A clear oil was obtained, yield 55%. ^{1}H NMR (500 MHz, Deuterium Oxide) δ 5.82 (d, J = 1.5 Hz, 1H), 5.41 (s, 1H), 4.11 (dd, J = 8.7, 3.6 Hz, 1H), 2.74 (dd, J = 14.6, 3.6 Hz, 1H), 2.45 (dd, J = 14.6, 8.6 Hz, 1H). ^{13}C NMR (126 MHz, D_2O) δ 180.9, 176.1, 142.2, 123.0, 123.0, 71.9, 37.9. HRMS (ESI-): *m/z* 159.0301 $[M-H]^-$; calculated for $C_6H_8O_5$ $[M-H]^-$ 159.0299

*Dimethyl (E)-4-oxopent-2-enedioate (**11**):* Compound **9** (1.0 g, 4.84 mmol) was dissolved in 20 mL of CCl_4 and acetonitrile (1:1) in a 100 mL round bottom flask. An aqueous solution of sodium periodate (4.14 g, 19.36 mmol) was added to the reaction mixture followed by the drop wise addition of an aqueous solution of Ruthenium tetroxide (0.5%, 10 mL, 0.48 mmol). The reaction mixture turned black. Completion of reaction was monitored by TLC. The reaction mixture was filtered through celite and the filtrate evaporated under reduced pressure. The residue was dissolved in dichloromethane (100 mL) and washed with sodium bisulfite (10% aqueous, w/v 50 mL) and brine (2x 50 mL). The organic layer was separated, dried over the sodium sulfate, filtered and evaporated under reduced pressure. The crude was dissolved in dichloromethane and purified by flash silica column chromatography eluting with 5% Ethyl acetate: hexanes giving a yellow crystalline solid, yield 40%. ^{1}H NMR (500 MHz, Chloroform-d) δ 7.63 (d, J = 16.1 Hz, 1H), 6.98 (d, J = 16.0 Hz, 1H), 3.94 (s, 3H), 3.85 (s, 3H).^{13}C NMR (126 MHz, $CDCl_3$) δ 182.3, 165.2, 161.1, 135.6, 134.2, 53.5, 52.7. HRMS (ESI +): *m/z* 173.0450 $[M + H]^+$; calculated for $C_7H_8O_5$ $[M + H]^+$ 173.0444.

(E)-4-Oxopent-2-enedioic acid (**12**)*:* Compound **11** (0.05 g, 2.18 mmol) was dissolved in 30 mL THF, an aqueous solution of lithium hydroxide (1.0 M, 4.5 mL) was added and stirred for 2 h at 20 °C. TLC was used to monitor for completion of the reaction. After 4 h solvent was evaporated under reduced pressure and residue was dissolved in 20 mL water, acidified to pH 4.0 with 10% HCl, and washed with ethyl acetate (50 mL) once. Water was removed by lyophilization. The solid obtained was dissolved in 25% acetonitrile/ water solution. The solution was passed through a Sep-Pak (1G) reverse phase column eluting with water followed by 20% acetonitrile/ water. Lyophilization of the pure fractions gave a clear oil, yield 40%. ^{1}H NMR (500 MHz, Deuterium Oxide) δ 6.48 (d, J = 1.9 Hz, 2H).

*Synthesis of Diethyl 2,2-difluoro-4-methylenepentanedioate (**13**):* This compound was synthesized according to the previously published literature.[17] Clear oil, yield 70%. ^{1}H NMR (500 MHz, Chloroform-*d*) δ 6.42 (s, 1H), 5.83 (s, 1H), 4.29 (q, J = 7.2 Hz, 2H), 4.21 (q, J = 7.2 Hz, 2H), 3.15 (t, J = 16.1 Hz, 2H), 1.33 (t, J = 7.2 Hz, 3H), 1.30 (t, J = 7.2 Hz, 3H). ^{13}C NMR (126 MHz, $CDCl_3$) δ 166.0, 139.8, 131.2, 130.8, 125.4, 125.2, 114.6, 69.9, 69.0, 63.0, 61.3, 60.7, 60.7, 36.4, 36.2, 36.0, 33.7, 30.9, 29.7, 28.3, 14.2, 14.1, 13.9.

2.1.6. Synthesis of diastereomeric triesters with (1S)-(-)-Camphanic acid chloride

To diester **1a** (10 mmol) dissolved in 100 mL of dichloroethane at 20 °C was added. N, N' diisopropylethylamine (DIPEA, 25 mmol) followed by catalytic 4-dimethylaminopyridine (DMAP, 1 mmol). The reaction mixture was stirred for 30 min at 20 °C and then (1*S*)-(−)-Camphanic acid chloride (10 mmol) was added. The reaction was monitored by TLC and after 6 h was complete. The solvent was evaporated under reduced pressure, the residue dissolved in 200 mL ethyl acetate, and washed with 10% HCl (50 mL) followed by brine (2x100 ml). The organic layer was separated, dried over magnesium sulfate ($MgSO_4$), filtered, and evaporated under reduced pressure. The residue was dissolved in dichloromethane and preabsorbed on silica and added to a column. Silica gel chromatography (¾‘ diameter, length column) eluting with 5–7% ethyl acetate: hexanes provided several fractions which were analyzed for diastereomeric purity. A second column was used to further purify the second eluting diastereomer.

*Diethyl(4S)-2-methylene-4-(((1S)-4,7,7-trimethyl-3-oxo-2-oxabicyclo [2.2.1]heptane-1-carbonyl)oxy)pentanedioate **15-(4S, 1S)**:* Obtained compound was an oil, isolated yield 40%. ^{1}H NMR (400 MHz, Chloroform-*d*) δ 6.29 (s, 1H), 5.68 (s, 1H), 5.35 (dd, J = 9.0, 4.6 Hz, 1H), 4.28 – 4.18 (m, 4H), 3.03 (dd, J = 14.5, 4.6 Hz, 1H), 2.83 (dd, J = 14.5, 9.1 Hz, 1H), 2.45 – 2.35 (m, 1H), 2.03 (ddd, J = 13.5, 9.3, 4.4 Hz, 1H), 1.93 (ddd, J = 12.8, 10.7, 4.5 Hz, 1H), 1.70 (ddd, J = 13.4, 9.4, 4.2 Hz, 1H), 1.30 (dt, J = 10.6, 7.2 Hz, 6H), 1.12 (s, 6H), 0.99 (s, 3H). ^{13}C NMR (101 MHz, $CDCl_3$) δ 178.0, 168.9, 166.7, 166.1, 135.1, 128.7, 90.9, 71.7, 62.0, 61.3, 55.0, 54.6, 53.6, 33.8, 30.7, 29.2, 16.7, 16.5, 14.3, 14.2, 9.8. HRMS (ESI +): *m/z* 414.2126 $[M + NH_4]^+$; calculated for $C_{20}H_{28}O_8$ $[M + NH_4]^+$ 414.2122. Specific rotation $[\alpha]^{20}_D$ = -13.36° $cm^3\ g^{-1}\ dm^{-1}$ (C = 1.035, ethyl acetate)

*Diethyl (4R)-2-methylene-4-(((1S)-4,7,7-trimethyl-3-oxo-2-oxabicyclo [2.2.1]heptane-1-carbonyl)oxy)pentanedioate **15-(4R, 1S)**:* Obtained compound was clear oil, isolated yield, 50%.[1]H NMR (400 MHz, Chloroform-*d*) δ 6.31 (s, 1H), 5.72 (s, 1H), 5.33 (dd, J = 8.9, 4.9 Hz, 1H), 4.23 (dq, J = 11.0, 7.2 Hz, 4H), 3.02 (dd, J = 14.6, 4.8 Hz, 1H), 2.86 (dd, J = 14.5, 8.9 Hz, 1H), 2.51 – 2.41 (m, 1H), 2.02 (ddd, J = 13.5, 9.3, 4.4 Hz, 1H), 1.91 (ddd, J = 13.0, 10.7, 4.5 Hz, 1H), 1.68 (ddd, J = 13.3, 9.3, 4.2 Hz, 1H), 1.30 (dt, J = 14.3, 7.1 Hz, 6H), 1.12 (s, 3H), 1.04 (d, J = 7.2 Hz, 6H). ^{13}C NMR (101 MHz, $CDCl_3$) δ 178.3, 168.8, 167.1, 166.2, 135.0, 129.0, 91.0, 72.0, 61.9, 61.3, 61.2, 55.1, 54.6, 33.7, 30.8, 29.0, 28.9, 16.7, 16.7, 16.6, 14.3, 14.2, 9.9. HRMS (ESI +): *m/z* 414.2127 $[M + NH_4]^+$; calculated for $C_{20}H_{28}O_8$ $[M + NH_4]^+$ 414.2122. Specific rotation $[\alpha]^{20}_D$ = +5.50° $cm^3\ g^{-1}\ dm^{-1}$ (C = 1.035, ethyl acetate)

3. 2.1.7 saponification of the diastereomeric triesters

Each of the camphanic acid chloride derived diastereoisomers (1 mol equiv.) was hydrolyzed with lithium hydroxide (1 mM aqueous, 4 mol equiv.) in 50 mL THF at 20 °C. TLC analysis demonstrated completion of reaction after 4 h. The solvent was evaporated under reduced pressure and residue dissolved in 50 mL water. The pH was adjusted carefully to pH 4.0 with 10% HCl (1.2 M). The aqueous solution was washed with ethyl acetate (1x50 mL), separated, and lyophilized. The residue was dissolved in 10% water/acetonitrile (10 mL) and loaded on Sep-Pak (5G) C-18 reverse phase cartridge. The desired compound was obtained by eluting in 20% water/acetonitrile. The pure fractions were concentrated under reduced pressure followed by lyophilization. These enantiomeric alcohols were further purified by C-18 4 μm preparative column (Agilent poreshell 6x150 μm 120) using on the Agilent Infinity 1260 II Infinity HPLC coupled with fraction collector and the appropriate fractions were combined, confirmed by HPLC and then lyophilized.

*(S)-2-Hydroxy-4-methylenepentanedioic acid (**16S**):* White crystalline solid, isolated yield 70%. ^{1}H NMR (500 MHz, Deuterium Oxide) δ 6.11 (d, $J = 1.3$ Hz, 1H), 5.65 (d, $J = 1.2$ Hz, 1H), 4.24 (dd, $J = 8.3$, 4.3 Hz, 1H), 2.85 – 2.77 (m, 1H), 2.55 (dd, $J = 14.5$, 8.4 Hz, 1H). ^{13}C NMR (126 MHz, D_2O) δ 179.8, 173.0, 138.5, 126.7, 71.1, 37.1. Specific rotation $[\alpha]^{20}_{D} = -5.59^{\circ}$ cm^3 g^{-1} dm^{-1} (C = 1.035, methanol) HRMS (ESI-): *m/z* 159.0295 [M−H]-; calculated for $C_6H_8O_5$ [M−H]- 159.0299

*(R)-2-Hydroxy-4-methylenepentanedioic acid (**16R**):* White crystalline solid, isolated yield 60%. ^{1}H NMR (400 MHz, Deuterium Oxide) δ 5.82 (d, $J = 1.6$ Hz, 1H), 5.41 (t, $J = 1.4$ Hz, 1H), 4.13 (dd, $J = 8.7$, 3.6 Hz, 1H), 2.77 (ddd, $J = 14.6$, 3.7, 1.4 Hz, 1H), 2.50 – 2.43 (m, 1H). ^{13}C NMR (101 MHz, D_2O) δ 181.1, 176.5, 142.6, 122.5, 72.0, 38.0. Specific rotation $[\alpha]^{20}_{D} = +3.21^{\circ}$ cm^3 g^{-1} dm^{-1} (C = 1.035, methanol). HRMS (ESI-): *m/z* 159.0294 [M−H]-; calculated for $C_6H_8O_5$ [M−H]- 159.0299.

3.1. Methods for evaluation of TET inhibition

3.1.1. Expression and purification of recombinant TET2^{CD}

The catalytic domain of TET2 was expressed and purified.[18] Briefly, TET2^{CD} cloned with *N*-terminal GST tag was affinity purified using AKTA purifier interfaced with GST Trap 5 mL column. The GST tag was cleaved and TET2^{CD} was further purified by gel filtration using (GST trap 5 mL sigma (catalogue # GE17-5131–01). The fraction containing recombinant TET2^{CD} were analyzed by stain free SDS-PAGE (BioRad cat #4568096) and pooled and concentrated using centiprep YM10™ to 10 mg/mL and stored at −80 °C for future use.

3.1.2. Dot-Blot assay for 5hmC/5mC quantification to measure TET inhibition

Cell permeable prodrug ester derivatives of our synthesized and procured compound library were tested at 25, 50, and 100 μM serial dilution concentration *in vitro* to test the ability of their corresponding diacids to inhibit TET dioxygenase activity. The inhibition of TET activity was determined by measuring the dose dependent decrease in global 5hmC using a dot blot assay.[18] The cells were treated for 12 h in the presence of 100 μM sodium ascorbate for genomic DNA extraction using the Wizard Genomic DNA Purification Kit (Promega, A1120). DNA samples were denatured in 0.4 M NaOH/10 mM EDTA for 10 min at 95 °C, neutralized with equal volume of 2 M NH_4OAc (pH 7.0), and spotted on a nitrocellulose membrane (pre-wetted in 1 M NH_4OAc, pH 7.0) in two-fold serial dilutions using a Bio-Dot® Microfiltration Apparatus (Bio-Rad, 1703938). The blotted membrane was air-dried, cross-linked by Spectrolinker™ XL-1000 (120 mJ/cm^2). Cross-linked membrane was blocked in 5% non-fat milk for 1 h at room temperature and incubated with anti-5hmC (Active motif, 1:5,000) or anti-5mC (Eurogentec, 1:2,500) antibody at 4 °C overnight. After 3x5 min washing with TBST, the membrane was incubated with HRP-conjugated anti-rabbit or anti-mouse IgG secondary antibody (Santa Cruz), treated with ECL substrate and developed using film or captured by ChemiDoc MP Imaging System (Bio-Rad). Membrane was then stained with 0.02% methylene blue in 0.3 M sodium acetate (pH 5.2) to ensure equal loading of input DNA.

3.1.3. Enzyme linked immunosorbent assay (ELISA) for TET2 activity

The ELISA assay of 5hmC for TET2 activity[19] was used for selected compounds as determined by the initial dot blot assay. The 96-well microtiter plate was coated overnight with 10 pmol avidin (0.66 μg, SIGMA A8706) suspended in 100 μL 0.1 M $NaHCO_3$, pH 9.6. Biotin labelled DNA substrate (10 pmol) was added for 2 h. The 60 bp duplex DNA substrate (forward strand: 5‘- ATTACAATATATATA-TAATTAATTATAATTAACGAAATTATAATTTATAATTAATTAATA-3‘ and reverse strand: 5‘-Bio-TATTAATTAATTATAAATTA-TAATTTmCGTTAATTAT AATTAATTATATATATATTGTAAT-3‘) was synthesized by IDT. Reactions were performed by adding 0.1 μM purified catalytic domain of TET2 in 100 μL reaction buffer containing 50 mM HEPES (pH 6.5), 100 mM NaCl, 1 mM DTT, 0.1 mM ascorbate, 25 μM $Fe(NH_4)_2(SO_4)_2$, 10 μM α-KG and different concentrations of inhibitor to each well for 2 h in 37 °C. Reaction was stopped by incubating with 100 μL of 0.05 M NaOH on a shaking platform for 1.5 h at room temperature. After brief washing with TBST, the wells were blocked with 2% BSA dissolved in TBST for 30 min, and then incubated with anti-5hmC antibody (Active motif, 39769, 1: 10,000) at 4 °C overnight. After washing with TBST, the wells were incubated with HRP-conjugated anti-rabbit secondary antibody (Santa Cruz). Signal was developed by adding TMB (SIGMA, T4444). Reaction was stopped by adding 2 M H_2SO_4 and absorbance at OD450 nm was read by Synergy H1 Hybrid Reader (BioTek).

3.1.4. Label free thermophoresis assay to measure the binding of TET2^{CD} of selected compounds

Binding interaction of **2a, 2b, 2c** with TET2^{CD} was monitored using label-free Microscale Thermophoresis (MST, NanoTemper).[18,20] Briefly, TET2^{CD} (0.5 μM) recombinant protein was mixed with different concentrations of **2a, 2b,** or **2c** in modified TET2 reaction buffer without α-KG containing 50 mM HEPES (pH 6.5), 100 mM NaCl, 1 mM DTT, 0.1 mM ascorbate and 25 μM $Fe(NH_4)_2(SO_4)_2$, loaded to capillary (NanoTemper, MO-Z022), and measured by the Monolith NT.115 (NanoTemper). Data were analyzed using MO. Affinity analysis V2.3 software using in built K_d model for data fitting and calculation of dissociation constant. GraphPad Prism 8.0.2 were used for plotting data.

3.1.4.1. LC-MS/MS analysis to probe TET2^{CD} modification. The recombinant purified TET2^{CD} (10 μM) was treated with **2a** (100 μM, 22 °C, 2 h) or mock in reaction buffer containing 50 mM HEPES (pH 6.5), 100 mM NaCl, 1 mM DTT, and 25 μM $Fe(NH_4)_2(SO_4)_2$. An aliquot of 30 μg of control or treated sample were reduced using dithiothreitol and alkylated using iodoacetamide and digested with trypsin (0.3 μg) and chymotrypsin (0.3 μg) and the digested samples were desalted using C18 Ziptips, dried in a SpeedVac and reconstituted in 1% acetic acid water solution for LC-MS/MS analysis on a UltiMate 3000 UHPLC system (ThermoFisher Scientific, Bremen, Germany) interfaced with an Orbitrap Elite hybrid mass spectrometer (Thermo Scientific, Bremen, Germany). The digest was analyzed using the data dependent multitask capability of the instrument acquiring full scan mass spectra using a Fourier Transform (FT) orbitrap analyzer to determine peptide molecular weights and collision induced dissociation (CID) MS/MS product ion spectra with an ion-trap analyzer at 35% normalized collision energy (NCE) to determine the amino acid sequence in successive instrument scans. The data were analyzed using Proteome Discoverer V2.3 (Thermo Fisher Scientific, Waltham, MA) with the search engine Sequest-HT which is integrated in the Proteome Discoverer software. The protein sequence database used to search the MS/MS spectra was the Uniprot *E. Coli* protein database containing 4454 entries plus the sequence of the recombinant protein TET2-CD with an automatically generated decoy

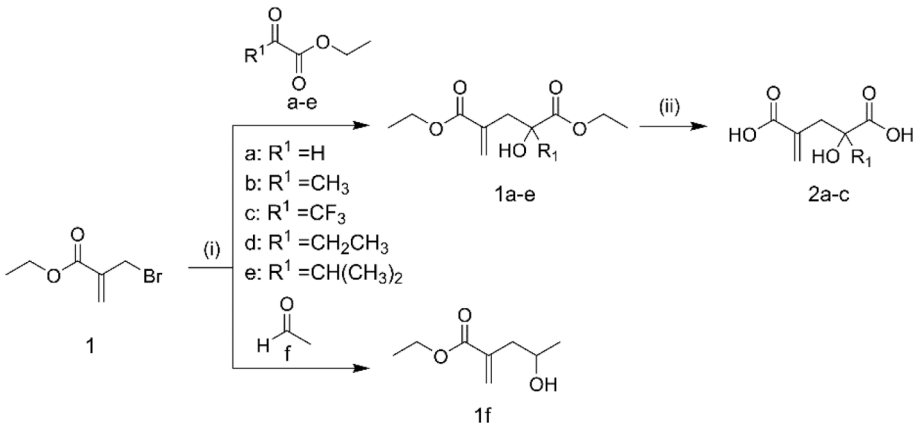

Scheme 1. Reagent and Conditions: (i) Zinc, acetic acid, CH_3CN, 20 °C; (ii) LiOH, THF: water (1:1), 20 °C.

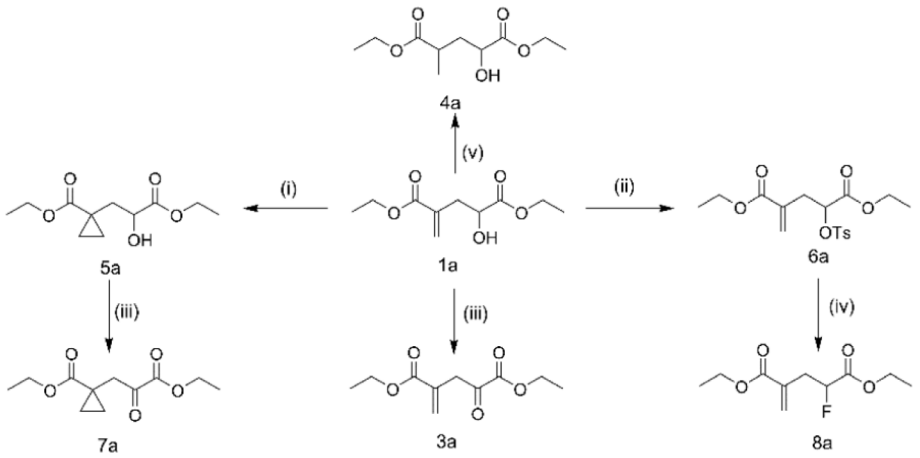

Scheme 2. Reagent and condition: (i) Diazomethane, DMSO, $COCl_2$; (ii) Dichloromethane, DMAP, TEA, TsCl, 20 °C; (iii) Dess-Martin oxidation, dichloromethane, 20 °C; (iv) CsF, k_{222}, CH_3CN, 20 °C; (v) $Pd(OH)_2$, 30 psi H_2, ethanol.

database (reversed sequences). For the trypsin digested samples, the protease was set to full activity trypsin with a maximum of 2 missed cleavages. For the chymotrypsin digested samples, the protease was set to semi activity chymotrypsin with a maximum of 4 missed cleavages. Oxidation of Methionine, carbamidomethylation of Cysteine, and a + 160.037 Da modification of Cysteine, Lysine and Arginine were set as dynamic modifications. The precursor mass tolerance for these searches was set to 10 ppm and the fragment ion mass tolerance was set to 0.8 Da. A false discovery rate (FDR) was set to 1% for both peptide and protein identification and calculated using the number of identified peptides/proteins from decoy database divided by the total number of identified peptides/proteins. The mass spectrometry proteomics data for amino acid residues modification upon treatment with **2a** have been deposited to the ProteomeXchange consortium via the PRIDE partner repository with the dataset identifier PXD024894.[21,22]

3.1.4.2. Computational docking of 2a and NOG. The crystal structure of TET2 catalytic domain ($TET2^{CD}$) in complex with α-KG pseudo substrate NOG and DNA oligo (protein data bank ID 4NM6) with Fe(II) was used for all docking simulations and structural activity analysis of **2a** by Glide running in Schrodinger Maestro environment. The complex was minimized and the binding site was analyzed in UCSF Chimera 1.8.[18] Ligand plot analysis were performed on the docked complex using LigPlot+ (https://www.ebi.ac.uk/thornton-srv/software/LigPlus/).

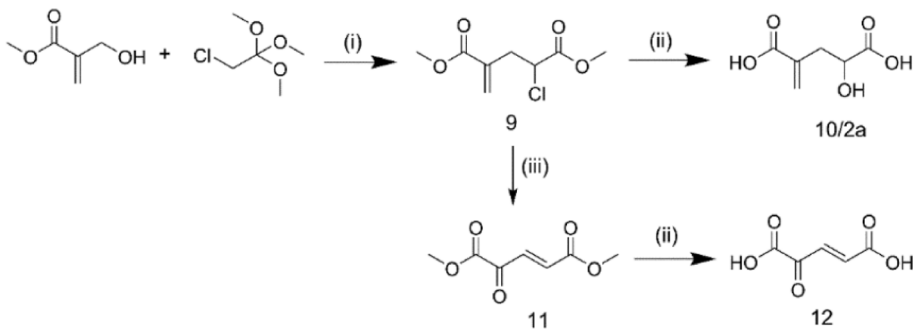

Scheme 3. Reagent and condition: (i) Toluene, acetic acid, reflux; (ii) LiOH (1.0 M aq.), THF; (iii) Ruthenium tetroxide, sodium periodate, 20 °C.

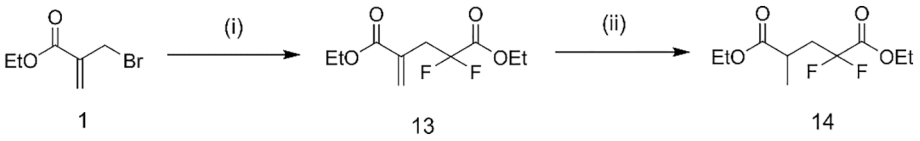

Scheme 4. Reagent and condition: (i) Zn, CuCN, $BrCF_2CO_2Et$, THF, 20 °C; (ii) Pd/C, Ethanol, 30 Psi, 20 °C.

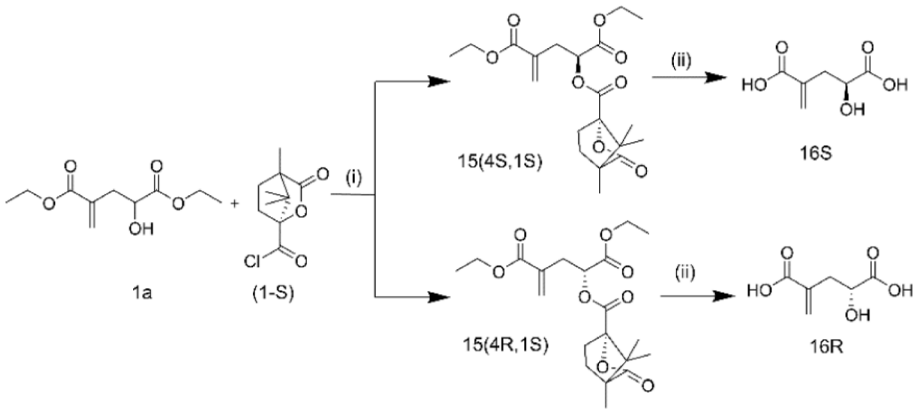

Scheme 5. Reagents and conditions (i). DMAP, DIPEA, dichloroethane, 20 °C (ii). LiOH, THF, H_2O, 20 °C.

4. Results and discussion

4.1. Chemistry

Our initial series of compounds were prepared by modified Barbier reaction of ethyl 2-(bromomethyl)acrylate (**1**) with substituted α-keto esters (**a-e)** which provided diethyl-2-hydroxy-4-methylenedicarboxylates **1a-f** as shown in scheme 1.[23] The corresponding dicarboxylic acids were then synthesized by treatment of the diesters with lithium hydroxide (LiOH) in THF: H_2O (1:1) at room temperature followed by careful acidification to pH 4.0. The diacids were purified by C-18 reverse phase chromatography with CH_3CN and

Table 1
Compound library of prodrug esters tested using the dot blot assay. THP1 cells at density of $0.3x10^6$/mL were treated with 25, 50 and 100 μM compounds for 12 h in the presence of 100 μM sodium ascorbate and the relative 5hmC/5mC quantification for TET enzyme inhibition (%) using dot blot were performed on genomic DNA. Data are means of inhibition from experiments performed at least three times. ND: not detected, if the inhibition is less than 5%. The TET enzyme inhibition assay considers that the ester prodrugs undergo ester hydrolysis during the course of the *in vitro* exposure (12 h) to the THP1 cells.

		TET Enzyme inhibition (5hmC/5mC) %					TET Enzyme inhibition (5hmC/5mC) %		
Entry	Structure	25	50	100 μM	Entry	Structure	25	50	100 μM
ASTA:22879		ND	ND	ND	3a	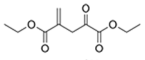	ND	27	44
A	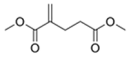	ND	7	22	4a	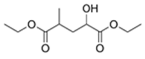	ND	14	41
DMKG	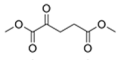	ND	ND	ND	5a	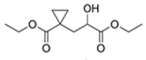	ND	ND	ND
DMOG	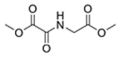	56	62	64	7a	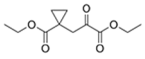	19	29	33
DMF	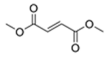	ND	21	33	8a	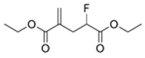	9	11	41
DMS	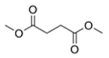	ND	7	15	9	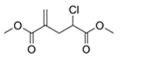	40	54	66
DMHG	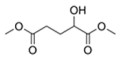	9	18	29	11	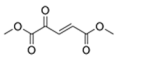	7	17	34
1a	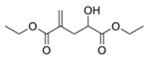	55	68	73	13	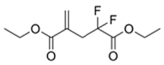	12	20	29
1b	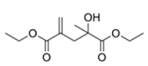	54	71	80	14	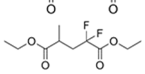	14	9	22
1c	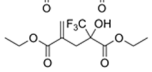	49	67	79	21a	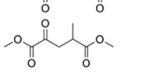	ND	ND	ND
1d	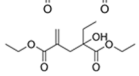	29	45	48	22b	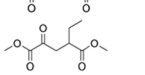	ND	ND	ND
1e	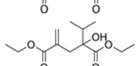	17	37	43	1f	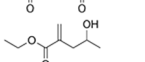	15	27	47

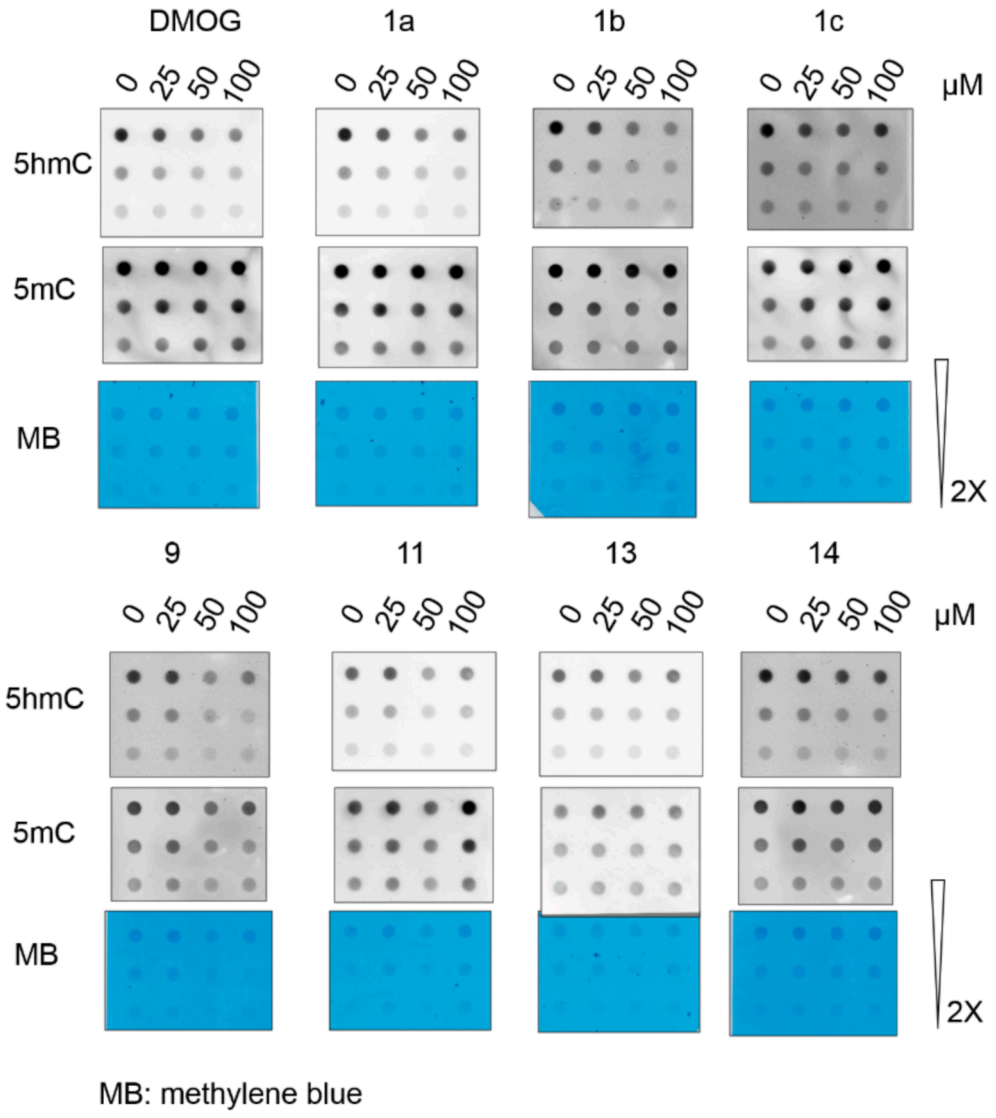

Figure 2. Selected prodrug esters tested using the dot blot assay. THP1 cells at density of $0.3x10^6$/mL were treated with 25, 50 and 100 μM compounds for 12 h in the presence of 100 μM sodium ascorbate and the relative 5hmC/5mC quantification using dot blot were performed on genomic DNA.

H_2O.

In order to evaluate a more detailed effect of the C-4 orthogonal methylene group, we prepared the reduced double bond derivative **4a** by $Pd(OH)_2$ catalyzed hydrogenation and the cyclopropane analog **5a** via diazomethane insertion from **1a**, respectively (Scheme 2).[17,16] The combined effects of the C-4 methylene and the C-2 hydroxy substituent were considered by replacing the hydroxy group with fluoride via the tosylate intermediate **6a** to provide **8a** (Scheme 2).[17] For determination of the hydroxy group significance, we used Dess-Martin oxidation based procedures to oxidize the secondary hydroxy group of **1a** to the corresponding ketone **3a** and that of **5a** to ketone **7a** (Scheme 2).

Two other ester compounds **9** and **13** (Scheme 3, 4) were prepared as well to determine possible effective replacements for the C-2 hydroxy group in our 4-methylene-2-disubstituted pentanedicarboxylates. Scheme 3 illustrates the synthesis of the 2-Cl derivative **9** and the attempted synthesis of its corresponding diacid from commercially available methyl 2-(hydroxymethyl)acrylate and the orthoester, 2-chloro-1,1,1-trimethoxyethane.[24] Oxidation of chloride **9** provides the α-keto ester **11** directly as under the reaction conditions the C-2 chloride substituent eliminates. The diacid **12** follows by saponification. Saponification of **9** provided **2a** directly as the basic conditions convert the 2-Cl substituent to a hydroxy group. Scheme 4 uses the condensation reaction of acrylate **1** and ethyl 2-bromo-2,2-difluoroacetate to prepare the C-4 methylene C-2 difluoro analog **13** followed by catalytic hydrogenation which provides the C-4 methyl derivative **14**.[17]

The individual enantiomers of the racemic mixture of diacid-alcohols **2a** were also prepared to determine if stereochemistry of the C-2 hydroxy substituent had an effect on activity. The racemic mixture **1a** was subjected to reaction with (1*S*)-(-)-camphanic acid chloride to afford the diastereomeric triesters **15(4R,1S)** and **15(4S,1S)**.[25] The diastereomers were separated by careful silica gel chromatography and then individually converted to their corresponding diacid forms **16R** and **16S** by saponification with LiOH (Scheme 5). The assignment of stereochemistry for the chiral center in the each of the camphenic acid esters **15-(4R,1S)** and **15-(4S,1S)** is based on comparison of their Circular Dichroism (CD) spectra with S-2HG shown in supporting information (**Figure S-1**). Triester **15-(4S,1S)** absorbs the circular polarized light in the same direction as S-2HG. Furthermore, the optical rotation data for the camphenic acid derived triester **15-(4S,1S)** being $[\alpha]^{20}_D = -13.36°$ $cm^3\ g^{-1}\ dm^{-1}$ (C = 1.035, ethyl acetate) is in the same rotation direction as its corresponding alcohol diacid **16-(2S)** $[\alpha]^{20}_D = -5.59°$ $cm^3\ g^{-1}\ dm^{-1}$. The data for **15-(4R,1S)** is + 5.50° $cm^3\ g^{-1}\ dm^{-1}$ and its corresponding alcohol diacid **16-(2R)** is + 3.21° $cm^3\ g^{-1}\ dm^{-1}$.

The synthesis of α-KG derivatives containing either a methyl or ethyl

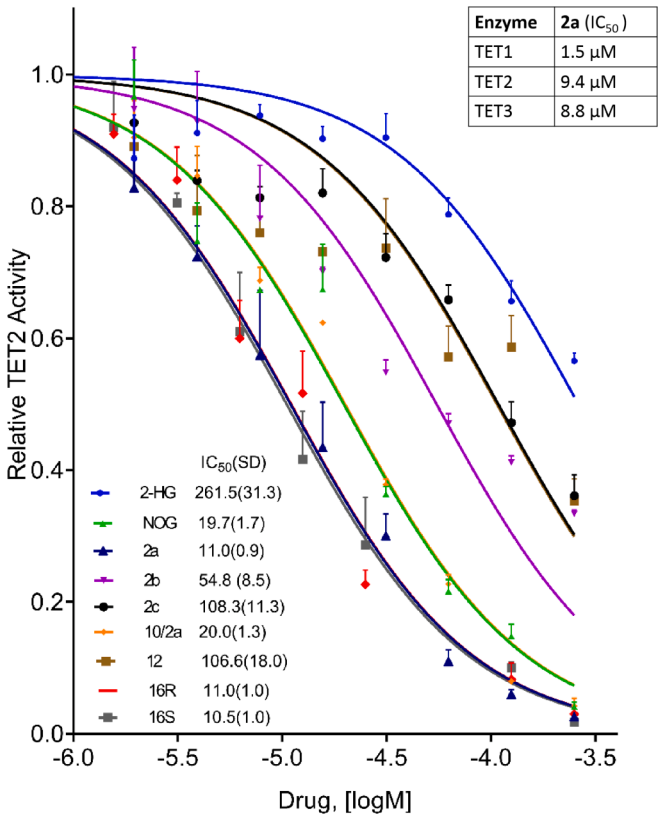

Figure 3. Dose dependent inhibition of TET activity (5hmC/5mC) of selected diacid compounds in cell free condition. Catalytic domains of recombinant TET2 was incubated with diacid separately in the presence of α-KG and Fe(II), and 5hmC was monitored by ELISA using anti- 5hmC antibodies.

substituent at C-4 were accomplished as published in the literature.[24] These compounds **21a, 21b** were synthesized and screened for their activity.

4.2. Structure activity relationships (SARs)

Initial empirical TET-inhibitory activity of our compound library were accessed as their cell permeable prodrug ester forms in TET-proficient THP1 (AML) cells at three different concentrations (Table 1, Figure 2, **S-2**). Our SAR discussion/comparisons are based on the assumption that the ester prodrugs undergo ester hydrolysis forming their corresponding diacids/acids during the course of the *in vitro* exposure (12 h) to the THP1 cells. The TET-dependent oxidation product of 5mC containing DNA were determined by dot blot analysis.[18–19] Compounds **1a-f** which contain the C-4 methylene substituent and a secondary or tertiary (-R^1) hydroxy group showed good potency and a concentration dependence. Two commercially procured compounds such as entry **A** (Toronto chemical research, D495948) and dimethyl-2-hydroxyglutarate (**DMHG**) which do not contain both features of the 2-hydroxy substituent and the C-4 methylene respectively were considerably less inhibitory. Reduction of the orthogonal methylene group **4a (**this produces diastereomers) or its conversion to a cyclopropane ring **5a** also reduced the level of inhibition. Tertiary alcohol derivatives with bulkier C-4 substitution, (ethyl) **1d** or (isopropyl) **1e** were slightly less active than NOG and the analogues **1a-c**. 2-substituted-4-methylene pentanedicarboxylate esters with C-2 fluoro or difluoro substitution (**8a**, **13** respectively) were less active than their hydroxy **1a** derivative. The C-2 fluoro or difluoro substituents of these diesters could possibly exhibit lower activity due to their fluorine-based hydrogen bonding acceptor properties which may effect different energy minimized conformations in the catalytic site or alteration of their ester hydrolysis rates. Of course, we must consider that the 2-hydroxy substituents of **1a-c** can act in both capacities as H bond acceptor or donors. The 2-chloro-4-methylene derivative **9** shows good activity consistent with **1a**. We surmise that the **9** is getting hydrolyzed to **1a** under assay conditions. Derivative **1f** which lacks the second carboxylate group but contains the methylene and hydroxy substituents has reduced activity compare to **1a-d**. The α-KG based compounds such as dimethyl-2-ketoglutarate and **21a, b** with alkyl substituents at C-4 but containing the C-2 keto functionality showed no inhibition.

The SAR data appears to substantiate to some degree the ligand plot analysis shown in Figure 6 for **2a.** In **2a,** the 4-methylene functionality establishes an additional pi stacking interaction with **His1382** and the two sp^3 centers C-3 and the hydroxy bearing C-2 allow an energy minimized and flexible extended carbon chain that provides for a stronger carboxylate salt-bridge interaction with **Arg1261**. These key interactions promote more potent inhibition, and are reinforced by the results demonstrated in the cell free ELISA and TET2 catalytic domain binding studies (Figures 3 and 4). Certainly, evaluation of a more substantial library of compounds along with extensive analyses of their in-silico docking in the catalytic site should shed considerable more light on what provides desirable modulation of TET activity. The preparation of different cell permeable acid-esters or diesters related to **1a** and efforts to more rigorously understand their pharmacology should be a focus of continuing studies.

4.3. TET2-inhibition in the cell free system

To confirm that the diester derivatives of selected compounds were effecting 5hmC levels via TET2 inhibition, we generated their corresponding diacids **2a**, **2b**, **2c**, **10/1a**, **12**, **16R** and **16S**. The dose response of these diacids in the cell free ELISA assay enables comparison to NOG and 2-HG. We observed a robust dose dependent reduction of the TET2-dioxygenase dependent oxidation product 5hmC, the decrease in the production determined as a ratio of 5hmC/5mC (Figure 3**).** The racemic diacid **2a** and its individual enantiomers, **16R** and **16S** demonstrated the most potent TET inhibition with 50% inhibitory concentrations of 11.0, 11.0, and 10.5 μM, respectively. These compounds are approximately 2 fold more potent than NOG (Figure 1**)**. Our data suggests that the in-vitro TET-inhibitory effects of **2a** in the cell free system is independent of the stereochemistry of the C-2 hydroxy chiral center since the IC_{50} for these two optical isomers **16R** (11.0 ± 1.0) and **16S** (10.5 ± 1.0) are similar to the racemic mixture **2a**. This is consistent with some reports pertaining to little difference in TET inhibition for the enantiomers of 2-HG, although these compounds demonstrate weak, low mM level inhibition.[10] However, we must consider that the in-vivo and cellular efficacy of 16R and 16S may still be different due to possible differential stability/metabolism of these compounds under physiological concentrations. The racemic tertiary alcohol derivatives **2b** (CH_3) and **2c** (CF_3) are less inhibitory than the secondary alcohol **2a**. Interestingly, the 2-keto-trans olefin diacid **12** shows inhibition with an IC_{50} of 106 μM. This compound could be considered in one sense a conformational restricted analog of the natural co-substrate α-KG and spur interest in the synthesis and evaluation of other rigid conformers. The racemic derivative **2a** was also determined to inhibit TET1, TET2 and TET3 with IC_{50} values of 1.5, 9.4 and 8.8 μM respectively (Figure 3 **insert**).[19]

4.4. TET inhibitors bind with recombinant $TET2^{CD}$

To further establish that 2-hydroxy-4-methylene pentanedicarboxylates **2a, 2b, and 2c** directly interact with the TET2 catalytic domain we performed the direct binding assay using the highly sensitive and label free Micro Scale Thermophoresis (MST) technique of $TET2^{CD}$ with **2a, 2b, and 2c**. Analysis of MST curves for the association of these 3 analogs with $TET2^{CD}$ were done using MO. Affinity software supplied with the instrument showed that **2a, 2b, and 2c** specifically bind to $TET2^{CD}$. The evaluation of binding constant performed using K_d model

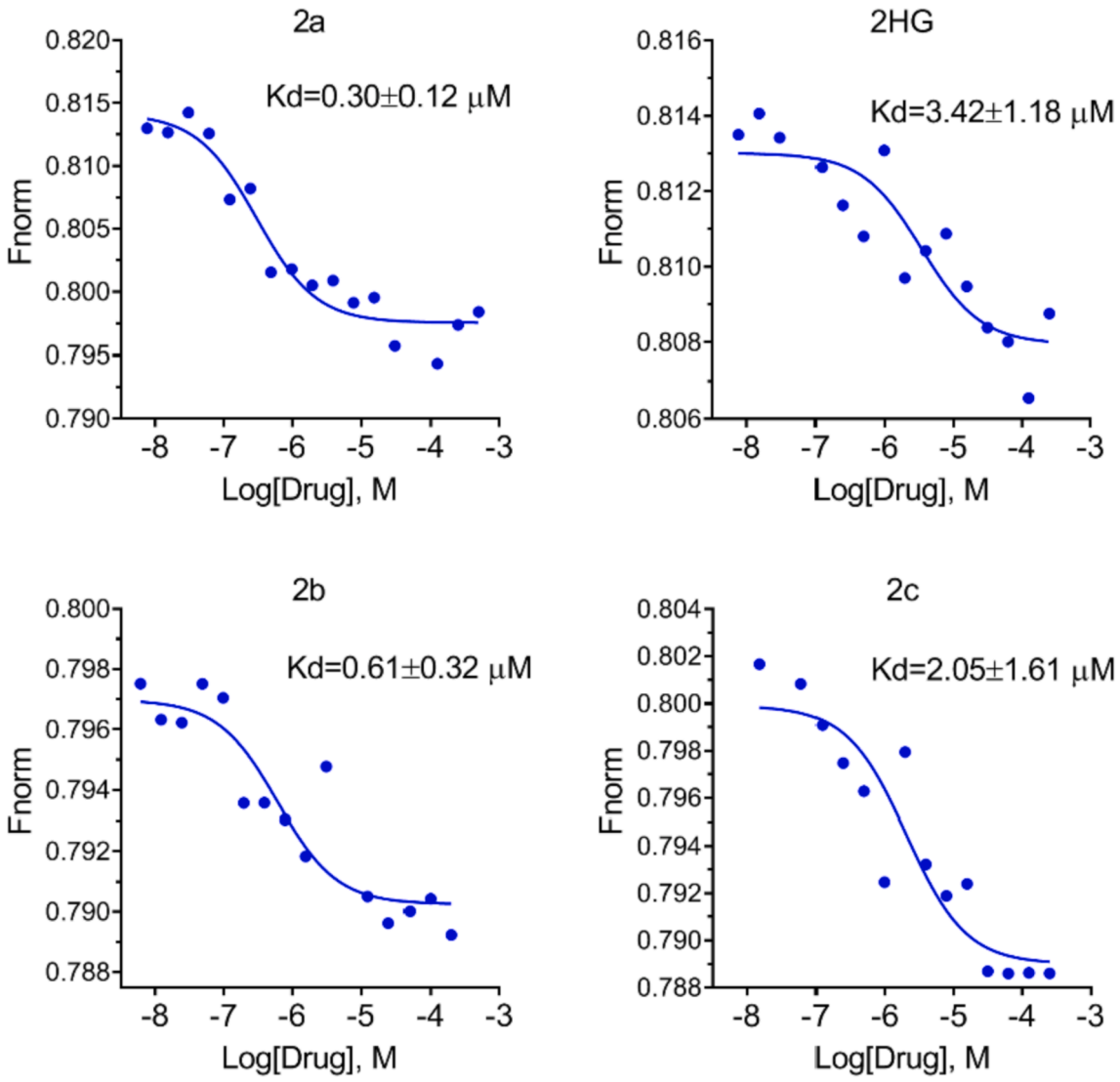

Figure 4. Binding affinities of diacid with recombinant purified human 1099–1936 Del-insert TET2^{CD}. Binding interaction of lead candidates with TET2^{CD} was monitored using label-free Microscale Thermophoresis (MST) on Monolith NT. Lable Free. The normalized MST signal (Fnorm) at different concentration is plotted. Data were analyzed using MO. Affinity analysis V2.3 software using built-in K_d model for data fitting and calculation of dissociation constant.

suggest a tight binding apparent in their dissociation constants of 0.3 μM, 0.61 μM, and 2.05 μM, respectively (Figure 4). This experimentally verified effect appears to also support our computational studies highlighting the differences in binding of NOG *vs* **2a** in the TET2^{CD}.

4.5. Reversible inhibition of TET-dioxygenases

Since **2a** has a methylene group in conjugation with its C-5 carboxylate, we considered that it could possibly irreversibly inactivate TET2 dioxygenase function by Michael addition of some of the key amino acid residues, i.e. cysteine, lysine and/or arginine in the catalytic domain.[26,27] We investigated this possibility in a designed experiment whereby we pre-incubated the TET enzyme with **2a** followed by increasing concentration of α-KG to restore the enzyme activity. First, using ELISA assay we established that α-KG (EC_{50} = 3.5 μM) saturates the dioxygenase activity of TET2^{CD} at 20 μM (Figure. 5A). If TET2^{CD} is irreversibly modified by **2a**, the activity should not be restored by addition of any excess amount of α-KG in the saturated concentration range. Given the 50% inhibitory concentration of **2a** is 11 μM for TET2^{CD}, in the ELISA assay, we used>100-fold molar excess of **2a** (12.5 μM), over TET2^{CD} protein (100 nM) followed by increasing concentration of α-KG (Figure. 5B). Consistent with the idea of reversible inhibition by **2a**, we observed that addition of increasing concentration of α-KG to TET2^{CD}-**2a** complex restored back dioxygenase activity in a dose dependent manner (Figure. 5B). The reversible nature of TET-inhibition was further confirmed by LC-MS/MS experiments, where no modification of Michael donor amino acid residues of TET2 was observed. In the experiment, TET2^{CD} was pre-incubated with 10-fold molar access of **2a** for 2 h, followed by in solution protein digestion and mass spectrometry analysis for TET2^{CD}. The resulting mass spectral data were analyzed for oxidation of methionine, carbamidomethylation of cysteine, and a + 160 Da modification of cysteine, lysine and arginine modifications, where 160 Da is the molecular weight of **2a**. Consistent with the reversible enzyme activity we did not observed covalent modification of + 160 Da of any peptide despite nearly 100% combined coverage of the peptides (Figure. 5C-D) suggesting a non-covalent reversible inhibitory mode of action of **2a** with TET2^{CD}.

4.6. Computational docking

The compounds, **1a** and **2a**, that we initially generated using the design concept of 2,4-disubstituted pentanedicarboxylates, showed

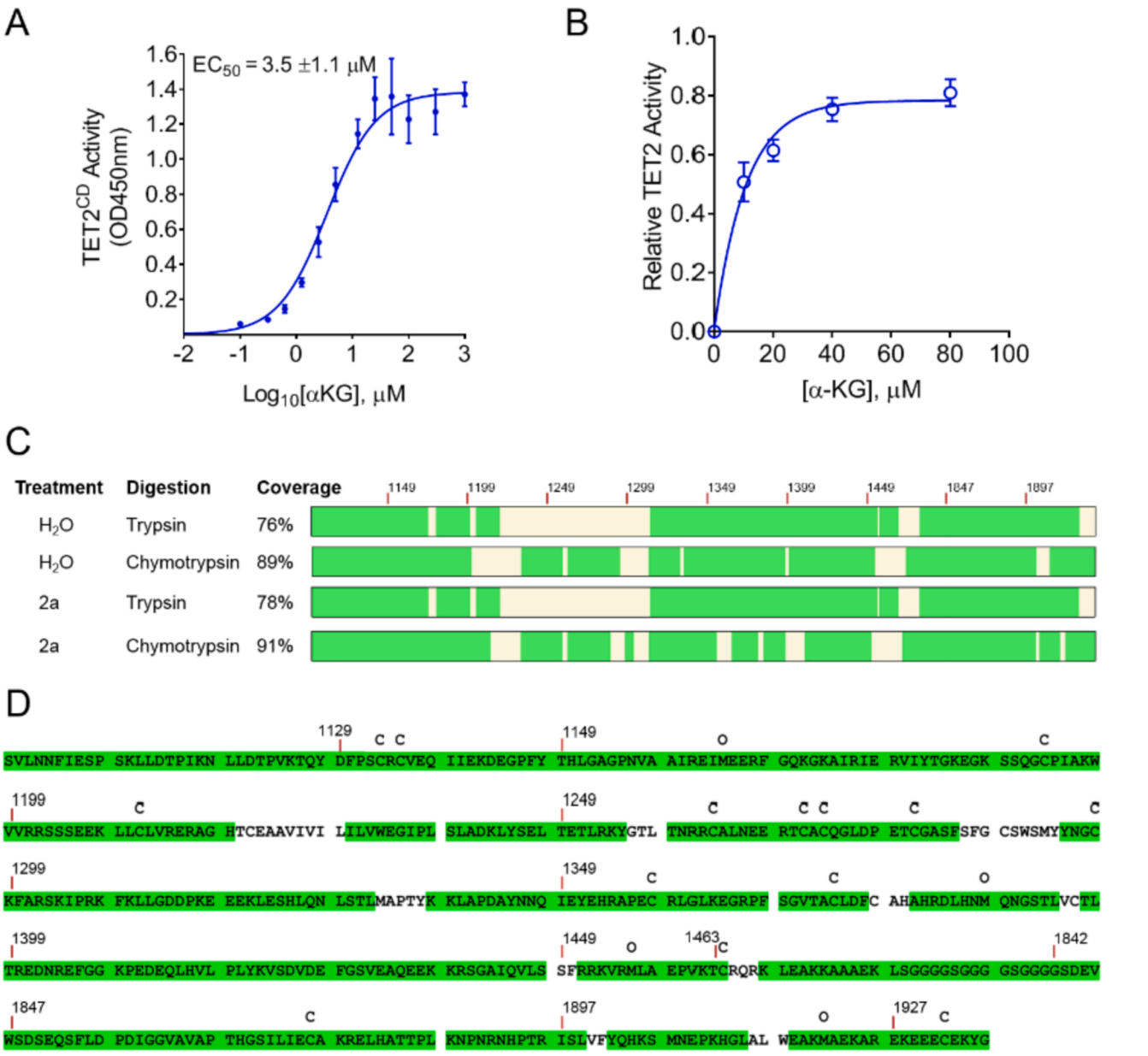

Figure 5. Reversible non-covalent inhibitor (**2a**) of TET-dioxygenases. (**A**): Dose response curve showing the TET2^{CD} dioxygenases activity response to α-KG, with an EC_{50} equals to 3.5 μM. ELISA assay was used to generate the curve. (**B**): Relative TET2 activities at different α-KG concentrations in the presence of 12.5 μM **2a** in the ELISA assay. The normalization of TET2 activity was performed to its controls. (**C-D**): The peptide coverage of TET2^{CD} (10 μM) in the presence and absence of **2a** (100 μM) with trypsin and chymotrypsin digestion followed by LCMS/MS analysis on OrbiTrap. C. Coverage map of TET2^{CD} D. Residue specific modifications in all observed peptides. C, Carbamidomethyl cysteine; O, Oxidation of Methionine.

robust competitive inhibition of TET-dioxygenase function (Table 1, Figure 2,**3**,**S-2**), and prompted us to perform docking simulations to compare to **NOG**. The docking simulation was performed using glide in schrodinger small molecule discovery suite followed by the energy minimization using CHARMM force field.[28,29] The docking model of our **2a** with TET2 showed that **2a** adopted a lower energy chain extended conformation than in comparison to NOG. Based on the LigPlot analysis, **2a** retained similar hydrogen bond interactions with **Arg1896**, **S1898**, **His1416**, **Arg1261** in TET2 compared with NOG (Figure 6). The van der Waals interactions between **2a** and TET2 were largely preserved compared with those between NOG and TET2 Although the coordination between the amide carbonyl group in NOG with Fe(II) is missing in **2a**, the vinyl group in **2a** establishes an additional pi stacking interaction with **His1382** and allows a stronger carboxylate salt-bridge interaction with **Arg1261** providing TET-specificity to **2a**. Only one oxygen atom in the olefin derivative **2a** interacts with Fe(II) instead of three oxygen atoms in NOG. In contrast to NOG, it is plausible that the inhibition of TET2 by **2a** may not require Fe(II) at the binding site and is therefore independent of Fe(II) concentration. This effect was subsequently confirmed by the ELISA assay. These observations provided continued encouragement and direction for our SAR studies to improve specificity and potency of TET inhibitors.

5. Discussion

There is an increasing number of reports of structurally diverse small molecules that are effective at inhibiting TET dioxygenase function via the catalytic domain. [13–15] However, attempts to develop small molecule probes for TET enzymes with cellular activity and specificity is quite challenging due to that there are over sixty α-KG-dependent human

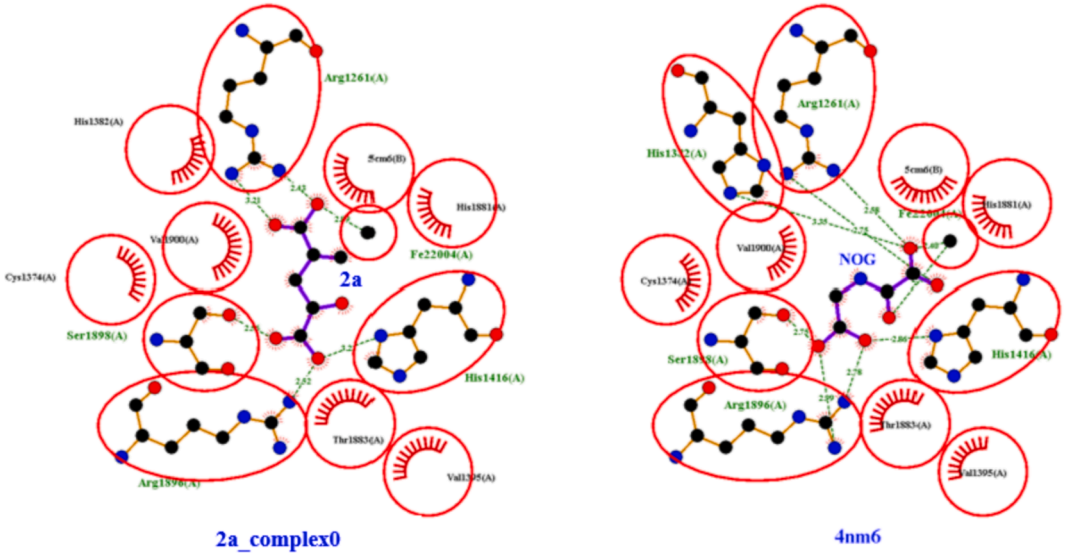

Figure 6. Ligand plot comparative analysis of lead molecule **2a** and NOG as complex with TET2. The docking simulation was performed in glide 3.1 followed by the energy minimization using CHARMM force field. Ligand plot was used for 2D projection of 3D structure. Dotted lines are H-bond.

oxygenases with similarity in active site fold.[30] Furthermore, the C-terminal catalytic domain of the three TET1-3 enzymes is highly conserved, yet these enzymes have different lineage specific functions, isoforms, interacting partners, and tissue distribution.[31] However, the focus of our studies developing inhibitors of TET2 dioxygenase function, and our results reported are significantly important amid evidence that transient inhibition of TET2 activity may be contextually beneficial therapeutically. TET2 is the most common somatically mutated gene of TET1-3 in myeloid neoplasia resulting in mono- or biallelic loss of function and affecting patients with acute myeloid leukemia, myelodysplastic syndrome, and myeloproliferative neoplasms. The TET2 gene is of particular importance for neoplastic evolution as it regulates the fate of hematopoietic stem and progenitor cells (HSCs) and is a founder lesion occurring early in the leukemic ontogenesis including its prominent role in clonal hematopoiesis of indeterminate potential (CHIP) as a precursor of myelodysplasia (MDS). The prevalence of CHIP increases with age as a likely cause for the elderly MDS demographics. Missense mutations and in-frame deletions occur in the catalytic domain of the TET2 protein. Nonsense and frameshift mutations can occur throughout the entire coding region, but they occur most frequently in the non-catalytic domain. Mutations in TET2 are generally inactivating regardless of their nature or location in the coding region of the gene. Our synthetic and computational studies reveal a unique binding interaction of our most studied inhibitor **2a** in the $TET2^{CD}$ which may be contributing to its selectivity determined thus far. The TET2 inhibitor **2a** does not inhibit 16 other α-KG/Fe(II) dependent enzymes tested to date.[19] However, **2a** inhibits TET1 slightly more potently than TET2-3, but approximately equipotent against the latter. Since TET2 is significantly mutated more often than TET1 and TET3, and our prodrug diester **1a** has demonstrated TET cellular inhibiting activity against THP1 cells (dot blot assay), it may be possible to exploit this therapeutically.[32] Recently, we have demonstrated a novel therapeutic strategy for selective targeting of TET2 mutant and TET-dioxygenase deficient cells in myeloid neoplasms with our lead compound **2a** exemplifying this approach. The apotheosis of this report demonstrates that our TET inhibitor **2a** suppressed the clonal evolution of TET2 mutant cells in murine models and TET2 mutated human leukemia xenografts with no detrimental effects on normal hematopoiesis.[19,32–33] Several other recent reports also suggest the therapeutic utility of TET2 inhibition in the treatment of cancer. For example, TET2 deletion may promote the sensitivity of anti-cancer treatment of p53-null tumor cells.[34] TET-dioxygenase deficient IDH1/2 mutant and TET2 mutant AML respond better to retinoic acid receptor activation.[35] Inhibiting TET2-dioxygenase function may prevent the exhaustion of hematopoietic stem cell progenitors, and therefore may have applicability in immunotherapy and CAR-T cell therapy.[36]

6. Conclusion

We have developed a potent and selective TET catalytic domain inhibitor that may constitute a new class of agents directed towards targeting TET2 mutant hyperplasia. Our most studied diester prodrug **1a** has cellular activity and its corresponding diacid-alcohol, **2a**, potently and reversibly inhibits TET2 dioxygenase function. Our SAR studies and computational efforts have provided important unique insights into the structural features of α-KG related small molecules that determine inhibition of TET catalytic domain function. Additional studies are planned to exploit these findings. Evaluation of a more substantial library of compounds along with extensive analyses of their in-silico docking in the catalytic site are ongoing and should shed considerable more light on what provides desirable modulation of TET activity. The preparation of cell permeable acid-esters or diesters related to **1a** and efforts to more rigorously understand their pharmacology are also a focus of continuing studies.

Author Contributions

A. Tiwari: Synthesis, SAR study design, NMR spectroscopy, writing and presentation of the paper, and editing. **Y. Guan:** Biological assays, formal analysis, data curation, writing biological components, and editing. **D. Grabowski:** Investigation, cell preparations, editing. **J.P. Maciejewski:** Conceptualization, biological experimental design, writing, editing. **B.K. Jha:** Computer aided drug design computation, Conceptualization of biological experimentation, writing, editing. **J.G. Phillips:** Synthesis, SAR study design, writing and presentation of the paper, editing.

Declaration of Competing Interest

JPM, BKJ, JGP, YG and ADT are inventors on the patent application filed for small molecule TET modulators.

Acknowledgment

We thank James Windak at the University of Michgan, for HRMS

analyses. We also thank the Cleveland Clinic Centre for Therapeutics Discovery and Case Western Reserve University Chemistry Department for access to their NMR instrumentation and other analyses. We appreciate the technical assistances of mass spectrometry from Drs. Belinda Willard and Ling Li in Proteomics and Metabolomics Core, Lerner Research Institute, Cleveland Clinic. Orbitrap Elite instrument used in the study was supported by NIH shared instrument grant S10RR031537 to Dr. Willard. This work was supported in parts, by grants from the NIH/NHLBI (R35HL135795 and R01132071), Leukemia and Lymphoma Society (LLS) TRP, and LLS SCOR and Taub Foundation to JPM and BKJ.

Appendix A. Supplementary data

Supplementary data to this article can be found online at https://doi.org/10.1016/j.bmc.2021.116141.

References

1 Scott-Browne JP, Lio C-WJ, Rao A. TET proteins in natural and induced differentiation. *Curr Opin Genet Dev*. 2017;46:202–208.
2 Strichman-Almashanu LZ, Lee RS, Onyango PO, et al. A genome-wide screen for normally methylated human CpG islands that can identify novel imprinted genes. *Genome Res*. 2002;12(4):543–554.
3 (a) Hon GC, Song CX, Du T, et al. 5mC oxidation by Tet2 modulates enhancer activity and timing of transcriptome reprogramming during differentiation. *Mol Cell*. 2014;56(2):286–297;
(b) Wang L, Ozark PA, Smith ER, et al. TET2 coactivates gene expression through demethylation of enhancers. *Sci Adv*. 2018;4(11):eaau6986.
4 Guan Y, Hasipek M, Tiwari AD, Maciejewski JP, Jha BK. TET-dioxygenase deficiency in oncogenesis and its targeting for tumor-selective therapeutics. *Semin Hematol*. 2021;58(1):27–34.
5 Goll MG, Bestor TH. Eukaryotic cytosine methyltransferases. *Annu Rev Biochem*. 2005;74:481–514.
6 Jaiswal S, Natarajan P, Silver AJ, et al. Clonal Hematopoiesis and Risk of Atherosclerotic Cardiovascular Disease. *N Engl J Med*. 2017;377(2):111–121.
7 Ferrone CK, Blydt-Hansen M, Rauh MJ. Age-Associated TET2 Mutations: Common Drivers of Myeloid Dysfunction, Cancer and Cardiovascular Disease. *Int J Mol Sci*. 2020;21(2):626.
8 Ko M, Huang Y, Jankowska AM, et al. Impaired hydroxylation of 5-methylcytosine in myeloid cancers with mutant TET2. *Nature*. 2010;468(7325):839–843.
9 McDonough MA, McNeill LA, Tilliet M, et al. Selective Inhibition of Factor Inhibiting Hypoxia-Inducible Factor. *J Am Chem Soc*. 2005;127(21):7680–7681.
10 Koivunen P, Lee S, Duncan CG, et al. Transformation by the (R)-enantiomer of 2-hydroxyglutarate linked to EGLN activation. *Nature*. 2012;483(7390):484–488.
11 Hu L, Li Z, Cheng J, et al. Crystal structure of TET2-DNA complex: insight into TET-mediated 5mC oxidation. *Cell*. 2013;155(7):1545–1555.
12 Islam K. The Bump-and-Hole Tactic: Expanding the Scope of Chemical Genetics. *Cell Chemical Biology*. 2018;25(10):1171–1184.
13 Sudhamalla B, Wang S, Snyder V, Kavoosi S, Arora S, Islam K. Complementary Steric Engineering at the Protein-Ligand Interface for Analogue-Sensitive TET Oxygenases. *J Am Chem Soc*. 2018.
14 Chua GNL, Wassarman KL, Sun H, et al. Cytosine-Based TET Enzyme Inhibitors. *ACS Med Chem Lett*. 2019;10(2):180–185.
15 Singh AK, Zhao B, Liu X, et al. Selective targeting of TET catalytic domain promotes somatic cell reprogramming. *Proc Natl Acad Sci*. 2020;117(7):3621–3626.
16 Liu X, Wang Y, Laurini E, et al. Structural Requirements of 2-Oxoglutaric Acid Analogues To Mimic Its Signaling Function. *Org Lett*. 2013;15(18):4662–4665.
17 Liu X, Chen H, Laurini E, et al. 2-Difluoromethylene-4-methylenepentanoic Acid, A Paradoxical Probe Able To Mimic the Signaling Role of 2-Oxoglutaric Acid in Cyanobacteria. *Org Lett*. 2011;13(11):2924–2927.
18 Guan Y, Greenberg EF, Hasipek M, et al. Context dependent effects of ascorbic acid treatment in TET2 mutant myeloid neoplasia. *Commun Biol*. 2020;3(1):493.
19 Guan Y, Tiwari AD, Phillips JG, et al. A Therapeutic Strategy for Preferential Targeting of TET2 Mutant and TET-dioxygenase Deficient Cells in Myeloid Neoplasms. *Blood Cancer Discovery*. 2021;1:1–16.
20 Sparks RP, Fratti R. Use of Microscale Thermophoresis (MST) to Measure Binding Affinities of Components of the Fusion Machinery. *Methods in molecular biology (Clifton. N.J.)*. 1860, 2019,:191–198.
21 Perez-Riverol Y, Csordas A, Bai J, et al. The PRIDE database and related tools and resources in 2019: improving support for quantification data. *Nucleic Acids Res*. 2019;47(D1):D442–D450.
22 Deutsch EW, Bandeira N, Sharma V, et al. The ProteomeXchange consortium in 2020: enabling 'big data' approaches in proteomics. *Nucleic Acids Res*. 2020;48(D1):D1145–D1152.
23 Blomberg, C., Synthetic Applications of the Barbier Reaction. In The Barbier Reaction and Related One-Step Processes, Springer Berlin Heidelberg: Berlin, Heidelberg, 1993; pp 14-74.
24 Alaux S, Kusk M, Sagot E, et al. Chemoenzymatic Synthesis of a Series of 4-Substituted Glutamate Analogues and Pharmacological Characterization at Human Glutamate Transporters Subtypes 1–3. *J Med Chem*. 2005;48(25):7980–7992.
25 Parker D. NMR determination of enantiomeric purity. *Chem Rev*. 1991;91(7):1441–1457.
26 Diehl KL, Kolesnichenko IV, Robotham SA, et al. Click and chemically triggered declick reactions through reversible amine and thiol coupling via a conjugate acceptor. *Nat Chem*. 2016;8(10):968–973.
27 Genest A, Portinha D, Fleury E, Ganachaud F. The aza-Michael reaction as an alternative strategy to generate advanced silicon-based (macro)molecules and materials. *Prog Polym Sci*. 2017;72:61–110.
28 Agyeman A, Jha BK, Mazumdar T, Houghton JA. Mode and specificity of binding of the small molecule GANT61 to GLI determines inhibition of GLI-DNA binding. *Oncotarget*. 2014;5(12):4492–4503.
29 Thakur CS, Jha BK, Dong B, et al. Small-molecule activators of RNase L with broad-spectrum antiviral activity. *PNAS*. 2007;104(23):9585–9590.
30 Islam MS, Leissing TM, Chowdhury R, Hopkinson RJ, Schofield CJ. 2-Oxoglutarate-Dependent Oxygenases. *Annu Rev Biochem*. 2018;87(1):585–620.
31 Melamed P, Yosefzon Y, David C, Tsukerman A, Pnueli L. Tet Enzymes, Variants, and Differential Effects on Function. *Front Cell Dev Biol*. 2018;6(22).
32 Cimmino L, Dolgalev I, Wang Y, et al. Restoration of TET2 Function Blocks Aberrant Self-Renewal and Leukemia Progression. *Cell*. 2017;170(6):1079–1095 e20.
33 Agathocleous M, Meacham CE, Burgess RJ, et al. Ascorbate regulates haematopoietic stem cell function and leukaemogenesis. *Nature*. 2017;549(7673):476–481.
34 Zhang J, Tan P, Guo L, et al. p53-dependent autophagic degradation of TET2 modulates cancer therapeutic resistance. *Oncogene*. 2019;38(11):1905–1919.
35 Garrett-Bakelman FE, Melnick AM. Differentiation therapy for IDH1/2 mutant malignancies. *Cell Res*. 2013;23(8):975–977.
36 Nobles CL, Sherrill-Mix S, Everett JK, et al. CD19-targeting CAR T cell immunotherapy outcomes correlate with genomic modification by vector integration. *J Clin Invest*. 2020;130(2):673–685.